

## MATHEMATICAL MODELING OF THE CuSn12 ALLOY SINTERING PROCESS

**Cristian ȘTEFĂNESCU, Petrică ALEXANDRU, Gheorghe GURĂU**

"Dunarea de Jos" University of Galati, Romania  
e-mail: cristian.stefanescu@ugal.ro

### ABSTRACT

*The purpose of this study is to use statistical methods, namely active experimental regression analysis, to forecast the size of the intergranular sintering bridge by mathematically modeling the sintering process as it is applied to the CuSn12 alloy powder. A first-order linear design method was used to characterize the correlation between the intergranular sintering bridge and the sintering parameters (temperature and sintering time). Using the free casting of the powder into graphite shapes, nine experiments were scheduled. Following sintering, the intergranular sintering bridge was evaluated metallographically using image analysis software. In order to optimize the sintering process, a regression equation has been established by mathematical modeling that predicts the size of the intergranular bridge with sintering parameters (temperature and time) with a high probability (>95%), within the experimental limits.*

**KEYWORDS:** CuSn12 powder, sintering intergranular bridge, bronze powder filter, mathematical model

### 1. Introduction

Powder metallurgy (PM) is a technique employed to manufacture products using metal powders. Refractory metals, high alloys, and particle composites are commonly produced by PM. These materials are challenging to manufacture using traditional metal processing methods. PM allows for the production of porous materials, such as bronze bearings and filters, with the porosity manipulated by the compaction and sintering processes. One of the benefits of the PM process is its cost-effectiveness in production, along with its ability to create intricate features and achieve high-quality surface finishes [1-3].

The PM processing variables are crucial aspects that directly impact the resulting material properties. Compaction pressure, sintering duration, and sintering temperature are a few of the processing variables. Agarwal et al. demonstrates in their review how conventional sintering affects the sintered density of premixed and pre-alloyed bronze (CuSn12) in relation to compaction pressure. Results showed that the sintered density trend for pre-alloyed and premixed bronze improved with increasing compaction pressure. Additionally, the sintered density of the pre-alloyed bronze was found to be

higher compared to the premixed bronze [4]. According to Keraghel *et al.*, the mechanical properties of the material can be enhanced by increasing the compaction pressure [5]. Adnan states that the qualities of porous bronze got better when the sintering time and temperature were increased [6]. In their study, Nakrod *et al.* examined the impact of compaction pressure and sintering time on a pre-alloyed bronze powder (CuSn10). Based on the findings, it was observed that the density of the samples rose as the compaction pressure increased [7]. Cojocaru et al. conducted a study on the impact of influencing the raw materials and sintering parameters on the porosity of sintered tin bronzes. They compared the use of mechanically pre-alloyed CuSn10 powders to a mixture of pure CuSn10 components, and varied the temperature and time of the sintering process. The relationship between these parameters has been mathematically defined [8].

The purpose of this study is to use statistical methods, namely active experimental regression analysis, to forecast the size of the intergranular sintering bridge by mathematically modeling the sintering process as it is applied to the CuSn12 alloy powder.

## 2. Experimental procedure

The experiments aimed to determine the correlation between the parameters of the sintering thermal treatment (sintering temperature,  $t$  [°C] and holding time at the sintering temperature,  $\tau$  [min]) and the size of the intergranular sintering bridges,  $x$  [ $\mu\text{m}$ ], in the case of products with high porosity, specifically filters made from CuSn12 powder through free pouring.

### 2.1. Materials used in research

Spherical powders of bronze, brass, nickel, stainless steel, titanium, silver, are commonly used to create metal filters through the sintering process. In the conducted researches, CuSn12 bronze powder was used, obtained by the atomization process. Granulometric characterization of CuSn12 powder (Figure 1) resulted from statistical analysis of data collected by measuring powder particles using a stereomicroscope (Table 1).

**Table 1.** Statistical analysis of the data obtained by measuring the spheroidal particles of the CuSn12 powder

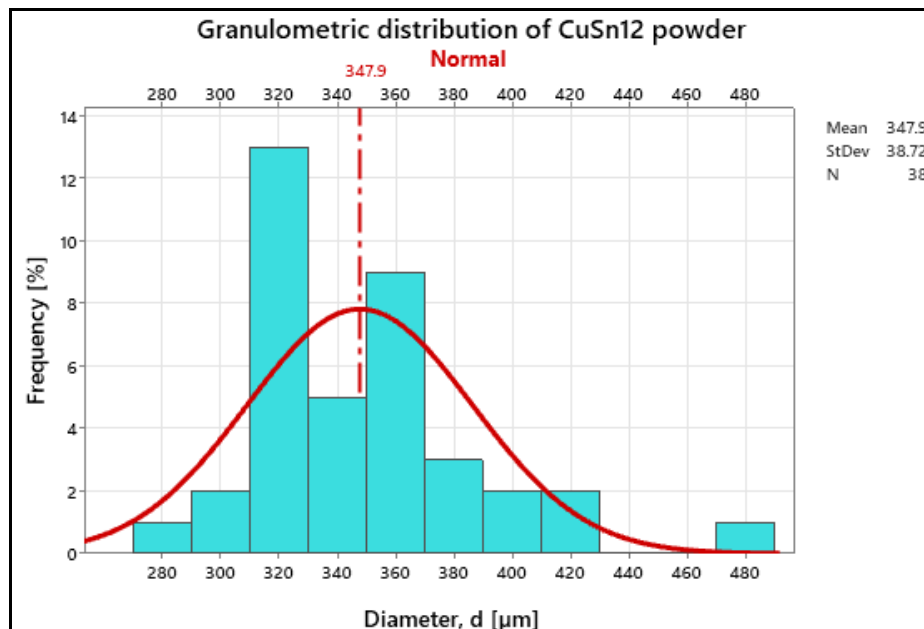
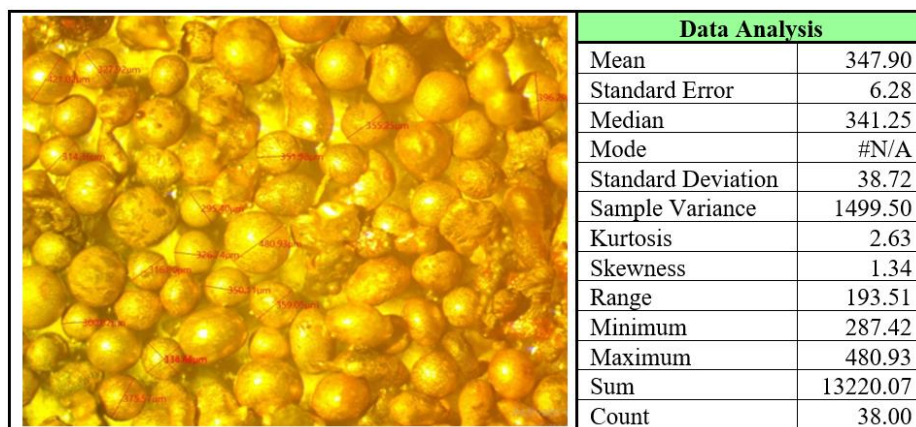


**Fig. 2.** Histogram of the granulometric composition of the CuSn12 powder

### 2.2. Forming of CuSn12 samples

The specimens were fabricated utilizing a graphite mould. The aforementioned approach

guaranteed the preservation of protective conditions during the sintering process, which involves a reducing environment. Additionally, the method facilitated the ease of shaping the material while

preventing the powder from welding to it. The mould was made up of two semi-cylindrical components. A cavity of the shape parallelepiped (38 x 4 x 1.5 mm) was machined into one of the components (Figure 2) [9].



**Fig. 2.** The mould with the two semi-cylindrical components used for the free casting of CuSn12 powder samples

### 2.3. Free casting in graphite moulds

To obtain the samples for this work, free casting in graphite moulds was opted upon. It is the simplest method for creating pieces with high porosity from powders that does not involve compression of the particles. Following the deposition of the powder into the mould cavity, a gentle vibration was induced by administering delicate impacts to the mould and the

excess was removed by scraping. Figure 2 shows the powder prepared for sintering before mounting the "cap" to close the mould cavity. The form was placed in an aluminium tube to preserve the graphite-generated reducing environment during sintering. Ceramic felt plugs were used to seal up the ends of the tube [9].



**Fig. 3.** The graphite mould with the powder that was ready to be sintered

### 2.4. Sintering

The production of sintering bridges (Figure 4) is a result of the following transport mechanisms: diffusion (surface, at grain boundaries, in volume), viscous flow, and evaporation-condensation [10].

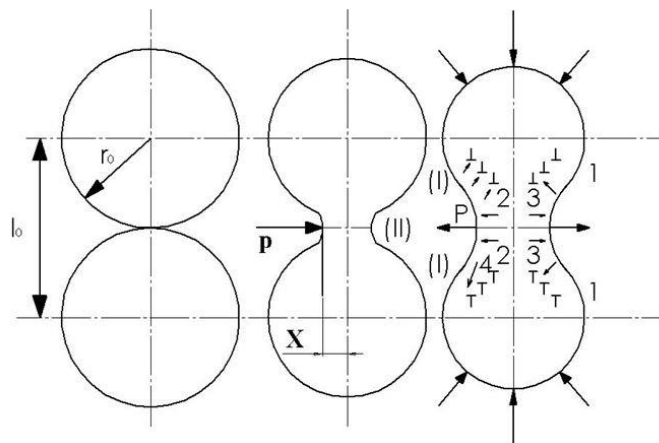


**Fig. 4.** Schematic illustrating how intergranular bridges form during the sintering process

The studies of the sintering process on regular geometric models of the ball-ball type, led to the establishment of the general form of the law of growth of sintering bridges (Kuczinski's equation) [10]:

$$\frac{x^n}{r^m} = k(t) \cdot \tau \quad (1)$$

where:

x - half-thickness of the sintering bridge;  
 r - radius of the powder particle;



$\tau$  - sintering time;  
 $k(t)$  - coefficient depending on the sintering temperature,  $t$ ;  
 $n, m$  - constants dependent on the type of material transfer mechanism during sintering.

The LENTON tubular enclosure electric furnace was used for sintering, and the heating regime was controlled automatically (Figure 5).



**Fig. 5.** The furnace LENTON used for sintering

The powder and sintered samples were examined and measured using a stereomicroscope (Carl Zeiss Jena) fitted with a TOUPCAM L3CMOS14000KPA digital camera. The software

used for image acquisition and processing was TouPCam TouPView [9].

Nine experiments were scheduled (3 temperatures x 3 durations). By using optical microscopy, the sizes of the intergranular bridges ( $2x$  [ $\mu\text{m}$ ]) and the particle diameters ( $d_1, d_2$  [ $\mu\text{m}$ ]) they connect were determined in the sintered samples (Figure 6).

An optical micrograph of one of the sintered samples ( $t = 880\text{ }^\circ\text{C}$ ,  $\tau = 60\text{ min}$ ) is shown in Figure 7.



**Fig. 6.** Appearance of a sintered sample

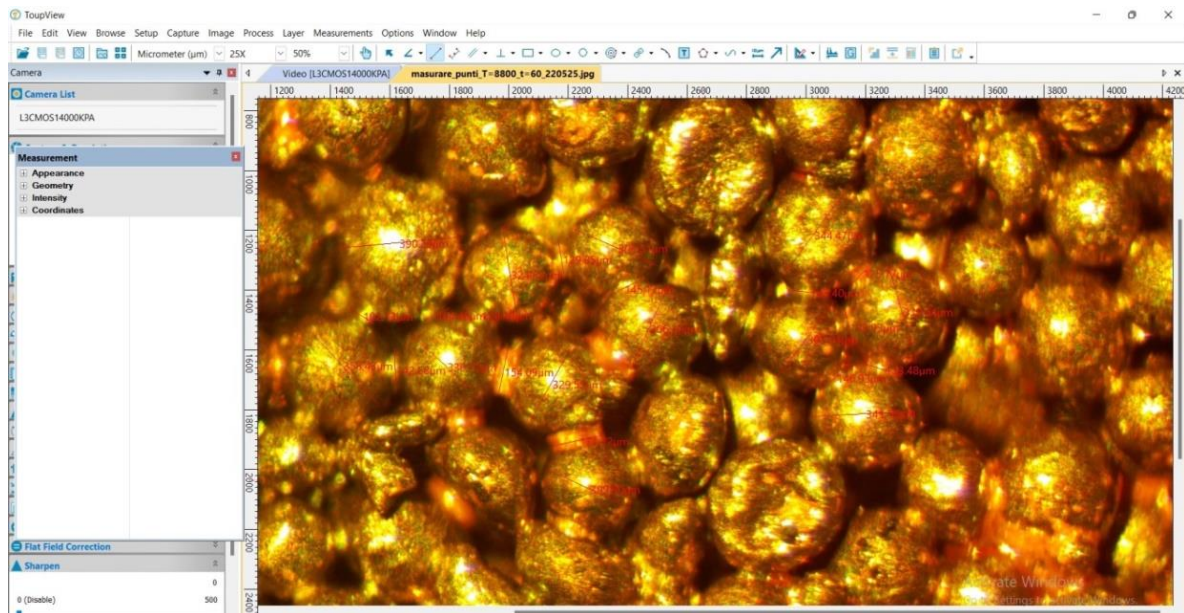


**Fig. 7.** Microscopic image of a sintered sample ( $t = 880\text{ }^\circ\text{C}$ ,  $\tau = 60\text{ min}$ )

For each of the 9 samples, corresponding to the experienced sintering regimes, 38 sets of measurements were made. A set includes the size of the bridge between two particles and their diameters.

Table 2 summarizes the results of the statistical analysis of the measurements taken on the 9 sintered samples in accordance with the specified experimental program.

**Table 2.** The average sizes of the intergranular bridges

Sample	Sintering parameters temperature, $t$ [°C]; time, $\tau$ [min]	Average values (intergranular bridge)
		$x$ [ $\mu\text{m}$ ]
1	$t = 880; \tau = 20$	61
2	$t = 880; \tau = 40$	65
3	$t = 880; \tau = 60$	67
4	$t = 900; \tau = 20$	72
5	$t = 900; \tau = 40$	76
6	$t = 900; \tau = 60$	82
7	$t = 920; \tau = 20$	82
8	$t = 920; \tau = 40$	73
9	$t = 920; \tau = 60$	84

### 3. Results and discussion

The objective of this research is to predict the size of the intergranular sintering bridge by mathematical modeling of the sintering process applied to CuSn12 powder. This will be done by using statistical methods, namely regression analysis by active experiment. The equation of the elaborated mathematical model is of the form:  $Y = f(z_1, z_2)$ .

**Table 3.** The correspondence between the values of the influence factors expressed in natural units and coded units

Factors Levels	Process temperature		Duration of the process	
	Natural units [°C]	Coded values	Natural units [min]	Coded values
Basic level	$u_{01} = 900$	$\frac{900 - 900}{20} = 0$	$u_{02} = 40$	$\frac{40 - 40}{20} = 0$
Interval of variation	$\Delta u_1 = 20$	0	$\Delta u_2 = 20$	0
Upper level	$u_{1s} = 920$	$\frac{920 - 900}{20} = +1$	$u_{2s} = 60$	$\frac{60 - 40}{20} = +1$
Lower level	$u_{li} = 880$	$\frac{880 - 900}{20} = -1$	$u_{2i} = 20$	$\frac{20 - 40}{20} = -1$

For the coded representation of the experiment, the following notations and symbols were used:

- o independent variables:
  - $z_1$  - sintering temperature,  $t$ , [°C];
  - $z_2$  - sintering time,  $\tau$ , [min];
- o Dependent variables (parameters to be optimized):
  - $Y_1$  – the intergranular bridge size,  $x$  [ $\mu\text{m}$ ], of Cu Sn12 alloy powder obtained after the sintering process.

### 3.1. Establishing the influencing factors and the parameter to be optimized

We considered the following sintering technological parameters as main influencing factors (independent variables):

1. sintering temperature –  $t$ , [°C];
2. holding time at sintering temperature –  $\tau$ , [min].

The intergranular bridge size,  $x$  [ $\mu\text{m}$ ], of Cu Sn12 alloy powder is taken into account as a design parameter to be optimized.

We established the experimental conditions as follows:

- for sintering temperature: - base level:  $u_{01} = 900$  °C;
- interval of variation:  $\Delta u_1 = 20$  °C;
- for the sintering time: - basic level:  $u_{02} = 40$  min;
- interval of variation:  $\Delta u_2 = 20$  min;

Table 3 shows the correspondence between the different levels of the factors expressed in natural values with those expressed in coded values, for the two factors used in the sintering process.

The link between the natural and coded values is achieved through correlation:

$$Z_1 = \frac{t - t_0}{\Delta t}; Z_2 = \frac{\tau - \tau_0}{\Delta \tau} \quad (2)$$

### 3.2. Determination of the first-order mathematical model

Since the influence of the two factors on the performance of the process ( $Y$ ) is being studied, a full

factorial experiment of type 2<sup>2</sup> was carried out. Table 4 presents the linear design matrix of the factorial experiment 2<sup>2</sup>.

Considering the function Y<sub>i</sub> as the analytical expression of the first-order model, it is of the form [11]:

$$Y_i = c_0 + \sum_{i=1}^k c_i z_i + \sum_{\substack{i=1 \\ j=1 \\ i \neq j}}^k c_{ij} z_i z_j \quad (3)$$

**Table 4.** The expanded linear design matrix of the 2<sup>2</sup> full factorial experiment

Factor	u <sub>0</sub>	Temperature t [°C] u <sub>1</sub>	Time, τ [min] u <sub>2</sub>	u <sub>1</sub> u <sub>2</sub>	Dependent parameter intergranular bridge, x[μm]
Code	z <sub>0</sub>	z <sub>1</sub>	z <sub>2</sub>	z <sub>1</sub> z <sub>2</sub>	Y <sub>1</sub>
Basic level, u <sub>0</sub>	-	900 (0)	40 (0)	-	-
Interval of variation, Δu <sub>j</sub>	-	20	20	-	-
Upper level u <sub>0</sub> +Δu <sub>0i</sub>	-	920 (+1)	60 (+1)	-	-
Lower level u <sub>0</sub> -Δu <sub>i</sub>	-	880 (-1)	20 (-1)	-	-
Exp.1	+1	+1/(920)	+1/(60)	+1	84
Exp.2	+1	-1/(880)	+1/(60)	-1	67
Exp.3	+1	+1/(920)	-1/(20)	-1	82
Exp.4	+1	-1/(880)	-1/(20)	+1	61
Exp.5	+1	+1/(920)	0/(40)	0	73
Exp.6	+1	-1/(880)	0/(40)	0	65
Exp.7	+1	0/(900)	+1/(60)	0	82
Exp.8	+1	0/(900)	-1/(20)	0	72
Exp.9	+1	0/(900)	0/(40)	0	76

For the present case, the linear function (4) has the following particular form:

$$Y_1 = c_0 + c_1 z_1 + c_2 z_2 + c_{12} z_1 z_2 \quad (4)$$

Equation (5) can be written in matrix form as follows:

$$Y = Z \cdot C \quad (5)$$

Where: Z is the matrix of experimental conditions;

$$Z = \begin{pmatrix} +1 & +1 & +1 & +1 \\ +1 & -1 & +1 & -1 \\ +1 & +1 & -1 & -1 \\ +1 & -1 & -1 & +1 \\ +1 & +1 & 0 & 0 \\ +1 & -1 & 0 & 0 \\ +1 & 0 & +1 & 0 \\ +1 & 0 & -1 & 0 \\ +1 & 0 & 0 & 0 \end{pmatrix}$$

- C - the column vector of the coefficients c<sub>i</sub>  
 $C = [c_0, c_1, \dots, c_n]^T$

T - the symbol for matrix transposition;

- Y - matrix of experimental results

-  $Y = [Y_1, Y_2, \dots, Y_n]^T$

-  $Y = [Y_1]^T$

-  $Y_1 = [84 \ 67 \ 82 \ 61 \ 73 \ 65 \ 82 \ 72 \ 76]$

Solving equation (5) using the Matlab R2016a software, the coefficients of the first-order model for property Y<sub>1</sub>, presented in Table 5, are obtained.

**Table 5.** The values of the coefficients of the first-order mathematical model

Y <sub>i</sub>	Y <sub>1</sub>
c <sub>0</sub>	73.55
c <sub>1</sub>	7.66
c <sub>2</sub>	3.00
c <sub>12</sub>	-1.00

Substituting in relation (4) we obtain:

$$Y_1 = 73,55 + 7,66z_1 + 3z_2 - z_1z_2 \quad (6)$$

By replacing the variables z<sub>i</sub> with relations (2) in the above equation, we obtain:

$$Y_1 = 73,55 + 7,66 \frac{(t - t_0)}{\Delta t} + 3 \frac{(\tau - \tau_0)}{\Delta \tau} - \frac{(t - t_0)(\tau - \tau_0)}{\Delta t \Delta \tau} \quad (7)$$

The final form of the first-order mathematical model is obtained by replacing the values of  $t_0$ ,  $\Delta t$ ,  $\tau_0$ ,  $\Delta \tau$  in equation (7).

Using equation (8) in Table 6 and Table 7 are presented the measured and calculated values of the property  $Y_1$ , as well as data necessary to verify the adequacy of the model by calculation.

$$Y_1(t, \tau) = 73,55 + 7,66 \frac{(t - 900)}{20} + 3 \frac{(\tau - 40)}{20} - \frac{(t - 900)(\tau - 40)}{20 \cdot 20}$$

$$Y_1(t, \tau) = 73,55 + \frac{7,66t - 6894}{20} + \frac{3\tau - 120}{20} - \frac{(t\tau - 40t - 900\tau + 36000)}{400}$$

$$Y_1(t, \tau) = \frac{(40 \cdot 73,55) + 20(7,66t - 6894) + 20(3\tau - 120) - t\tau + 40t + 900\tau - 36000}{400}$$

$$Y_1(t, \tau) = \frac{29420 + 153,2t - 137880 + 60\tau - 2400 - t\tau + 40t + 900\tau - 36000}{400}$$

$$Y_1(t, \tau) = \frac{-146860 + 193,2t + 960\tau - t\tau}{400}$$

$$Y_1(t, \tau) = -367,15 + 0,483t + 2,4\tau - 0,0025t\tau \quad (8)$$

**Table 6.** Measured and calculated values for  $Y_1$  ( $SP_{rez}$ )

Exp.	$Y_{1measured}$ [ $\mu\text{m}$ ]	$Y_{1calculated}$ [ $\mu\text{m}$ ]	$Y_{1measured} - Y_{1calculated}$ [ $\mu\text{m}$ ]	$(Y_{1measured} - Y_{1calculated})^2$ [ $\mu\text{m}$ ]
1	84	83.21	0.79	0.6241
2	67	69.89	-2.89	8.3521
3	82	79.21	2.79	7.7841
4	61	61.89	-0.89	0.7921
5	73	81.21	-8.21	67.4041
6	65	65.89	-0.89	0.7921
7	82	76.55	5.45	29.7025
8	72	70.55	1.45	2.1025
9	76	73.55	2.45	6.0025
<b>SUM (<math>SP_{rez}</math> – the sum of the squares of the residuals):</b>				<b>123.5561</b>

**Table 7.** Measured values and their average for  $Y_1$  obtained at the base level

No.	$Y_{01measured}$ [ $\mu\text{m}$ ]	$Y_{01medium}$ [ $\mu\text{m}$ ]	$Y_{01measured} - Y_{01medium}$ [ $\mu\text{m}$ ]	$(Y_{01measured} - Y_{01medium})^2$ [ $\mu\text{m}$ ]
1	73	73.60	-0.60	0.36
2	65	73.60	-8.60	73.96
3	82	73.60	8.40	70.56
4	72	73.60	-1.60	2.56
5	76	73.60	2.40	5.76
<b>SUM (<math>SP_{er}</math> – the sum of squared errors):</b>				<b>153.20</b>

### 3.3. Verification of model adequacy

A model is considered adequate if:

$$F_{ci} < F_T(f_{in}, f_{er}, 95\%) \quad (9)$$

where:

$- F_T(f_{in}, f_{er}, 95\%) = F_T(1,4,95\%) = 7.71$ ,  
 represents the value of the Fischer criterion adopted from the tables of the Fischer distribution [11];

$$- F_{ci} = -0,77$$

The values calculated with the relations above are centralized in Table 8.

**Table 8.** Sizes calculated to check the model's adequacy

Terms	Calculation relation	Calculated values
$SP_{rez}$ (Sum of squares of residuals)	Table 6	123.56
$PM_{rez}$ (Mean square of residuals)	$PM_{rez} = \frac{SP_{rez}}{f_{rez}} = \frac{SP_{rez}}{5}$	24.71
$SP_{er}$ (Sum of squared errors)	Table 7	153.20
$PM_{er}$ (Mean square of errors)	$PM_{er} = \frac{SP_{er}}{f_{er}} = \frac{SP_{er}}{4}$	38.30
$SP_{in}$ (Mean square of inadequacy)	$SP_{in} = SP_{rez} - SP_{er}$	-29.64
$PM_{in}$ (Mean square of inadequacy)	$PM_{in} = \frac{SP_{in}}{f_{in}} = \frac{SP_{in}}{1}$	-29.64
$F_{ci}$ (Value of Fischer's criterion)	$F_{ci} = \frac{PM_{in}}{PM_{er}}$	-0.77
$F_T(f_{in}, f_{er}, 95\%)$		7.71
<b>Concordance</b> $F_{ci} < F_T(1,4,95\%)$		<b>Concord</b>

### 3.4. Verification of the statistical significance of coefficients

The  $c_i$  coefficients are considered significant for which:  $F_{csi} > F_T(1, f_{rez}, (1 - \alpha)\%)$ .

In the present case:  $F_T(1, 5, 95\%) = 6,61$  [11], so:

$$F_{csi} = \frac{PM_{ci}}{PM_{rez}} > 6,61 \quad (10)$$

$PM_{ci}$  is the mean square of the coefficients that are calculated with the matrix relationship:

$$PM_{ci} = D_i(Z^t Y) \quad (11)$$

where:

-  $D_i$  is the diagonal matrix having as elements of the main diagonal the model coefficients, the other elements of the matrix being null,  $Z$  is transposed to the matrix of experimental conditions at the considered levels (-1,0,1);

-  $Y$  is the matrix of experimental results at the considered levels (-1,0,1).

For the equation of the mathematical model considered, the diagonal matrix  $D_i$ , has the following form:

$$D_1 = \begin{vmatrix} 73,55 & 0 & 0 & 0 \\ 0 & 7,66 & 0 & 0 \\ 0 & 0 & 3 & 0 \\ 0 & 0 & 0 & -1 \end{vmatrix}$$

The matrix calculation was performed using the MATLAB R2016a software, and the results are presented in Table 8.

**Table 9.** The values of the  $F_{csi}$  report

$c_i$	$c_0$	$c_1$	$c_2$	$c_{12}$
$F_{csi}$	1970.4614	14.259814	2.1853501	0.1618778

Analysing the  $F_{csi}$  report data from Table 9, shows that:

- The calculated values are strongly influenced by the terms which are preceded by the coefficients  $c_0$  and  $c_1$  for the equation of the mathematical model considered;
- The term which is preceded by the  $c_2$  coefficient has a relatively low influence;
- The term which is preceded by the  $c_{12}$  coefficient has a negligible influence.

Considering the above, the equation of the mathematical model written without the terms whose influence is negligible can be considered as viable. Thus, the form of equation (6), without the term preceded by the coefficient  $c_{12}$ , becomes:

$$Y_i = 73,55 + 7,66z_1 + 3z_2 \quad (12)$$

The transformation of equation (12) into an equation with natural variables is done starting from the conversion relations (2), relations that correspond to the data presented in Table 3 and we obtain the relation:



$$Y_1(t, \tau) = 73,55 + 7,66 \frac{(t - 900)}{20} + 3 \frac{(\tau - 40)}{20} = 73,55 + \frac{7,66t - 6894}{20} + \frac{3\tau - 120}{20}$$

$$= \frac{1471 + 7,66t - 6894 + 3\tau - 120}{20} = \frac{-5543 + 7,66t + 3\tau}{20}$$

$$Y_1(t, \tau) = -277,15 + 0,383t + 0,15\tau \quad (13)$$

Equation (13) represents the first-order mathematical model of the studied process valid for  $t = 880-920$  °C and  $\tau = 20-60$  min (the definition domain of the functions).

### 3.5. Results obtained

Table 10 and Table 11 show the values of the analysed factor ( $Y_1 = x$ ), calculated with the equation above, for different values of the sintering parameters ( $t$  and  $\tau$ ) and the graphs shown in Figures 8-13.

**Table 10.** Calculated  $Y_1 = f(t)$  for  $\tau = 20$  min;  $\tau = 40$  min;  $\tau = 60$  min

Intergranular bridge [ $\mu\text{m}$ ]		$Y_1 = f(t)$ $\tau = 20$ min			$Y_1 = f(t)$ $\tau = 40$ min			$Y_1 = f(t)$ $\tau = 60$ min		
		Temperature $t$ [°C]			Temperature $t$ [°C]			Temperature $t$ [°C]		
		880	900	920	880	900	920	880	900	920
Calculated	62.89	70.55	78.21	65.89	73.55	81.21	68.89	68.89	84.21	
Measured	61.00	72.00	82.00	65.00	76.00	73.00	67.00	82.00	84.00	
Graph	Figure 8			Figure 9			Fig. 10			

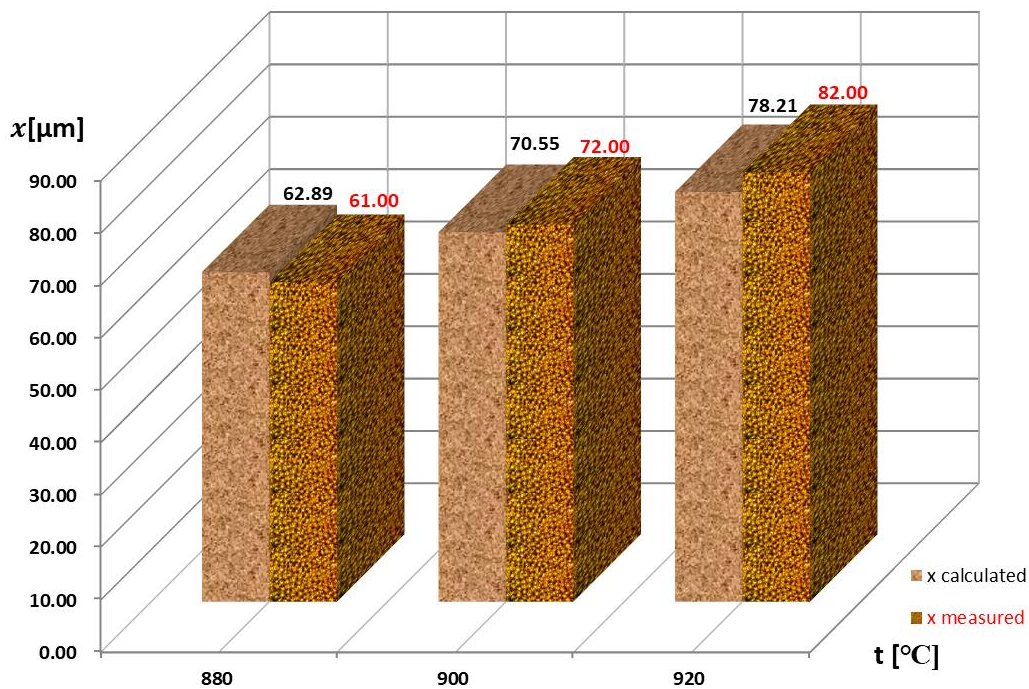


**Fig. 8.**  $Y_1 = f(t)$  for  $\tau = 20$  min

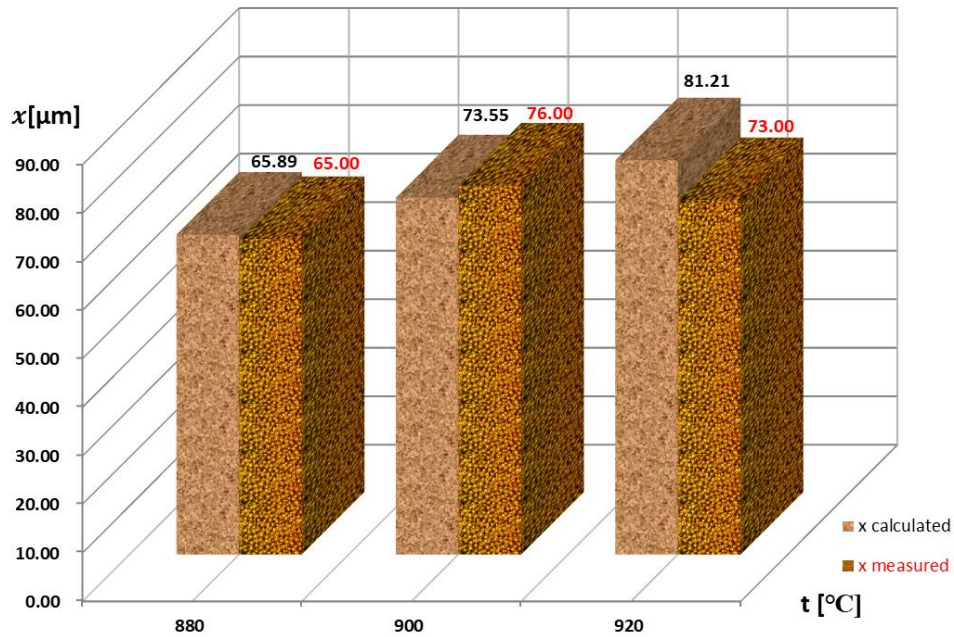


Fig. 9.  $Y_1 = f(t)$  for  $\tau = 40$  min

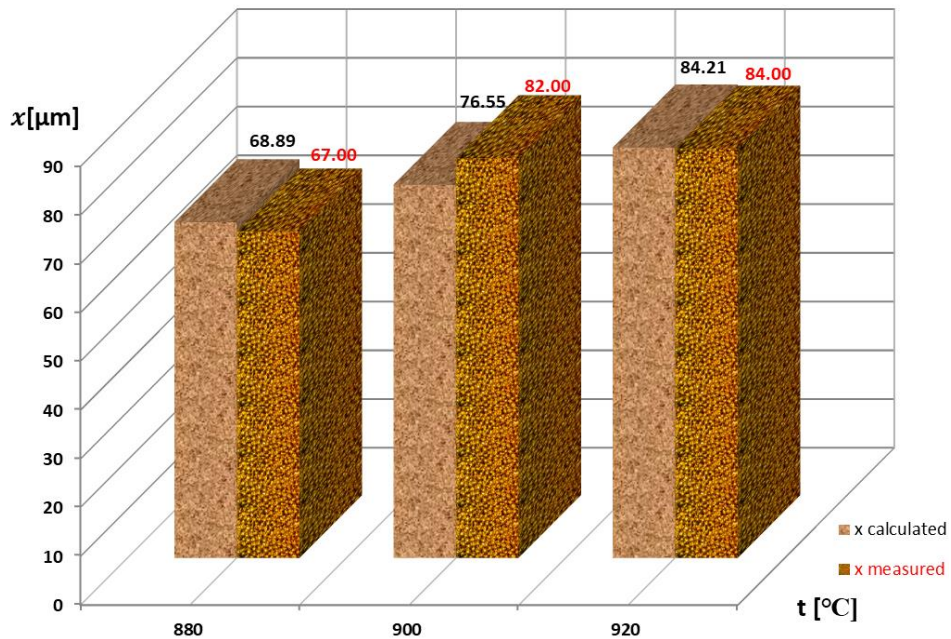


Fig. 10.  $Y_1 = f(t)$  for  $\tau = 60$  min

Table 11. Calculated  $Y_1 = f(\tau)$  for  $t = 880$  °C;  $t = 900$  °C;  $t = 920$  °C

Intergranular bridge [μm]		$Y_1 = f(\tau)$ $t = 880$ °C			$Y_1 = f(\tau)$ $t = 900$ °C			$Y_1 = f(\tau)$ $t = 920$ °C		
		Sintering time, $\tau$ [min]			Sintering time, $\tau$ [min]			Sintering time, $\tau$ [min]		
		20	40	60	20	40	60	20	40	60
Graph	Calculated	62.89	65.89	68.89	70.55	73.55	76.55	78.21	81.21	84.21
	Measured	61.00	65.00	67.00	72.00	76.00	82.00	82.00	73.00	84.00
Graph		Figure 11			Figure 12			Figure 13		

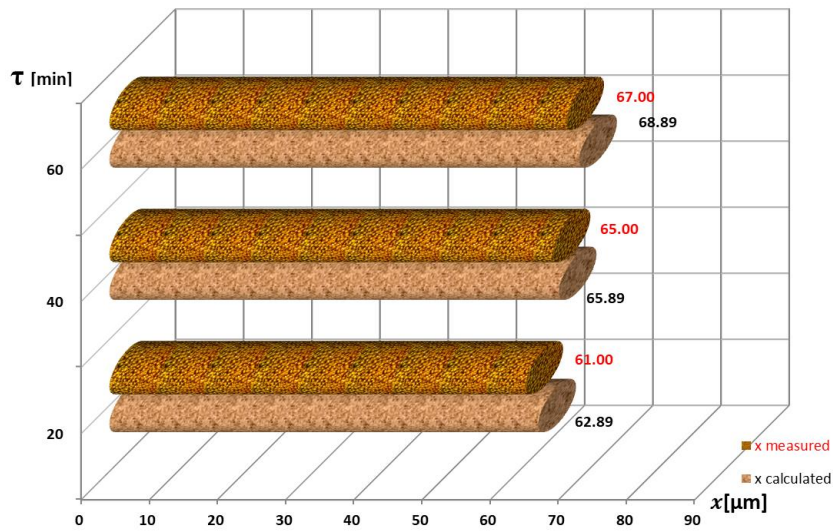


Fig. 11.  $Y_1 = f(\tau)$  for  $t = 880\text{ }^{\circ}\text{C}$

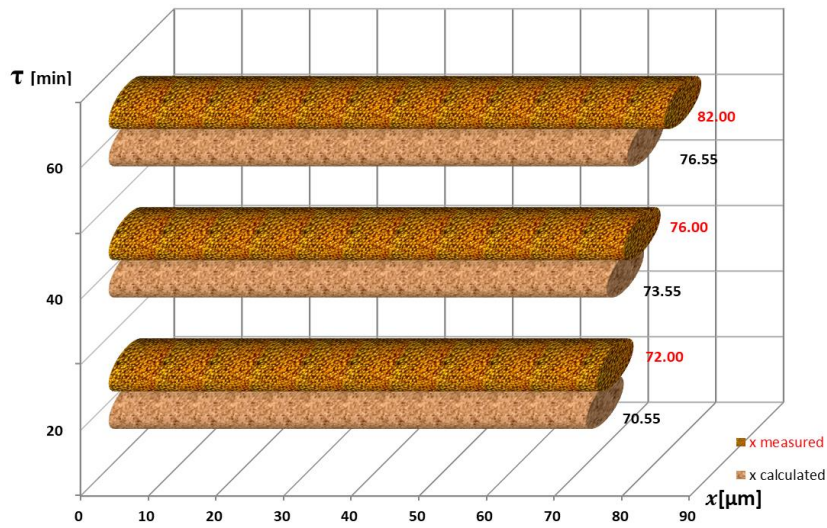


Fig. 12.  $Y_1 = f(\tau)$  for  $t = 900\text{ }^{\circ}\text{C}$

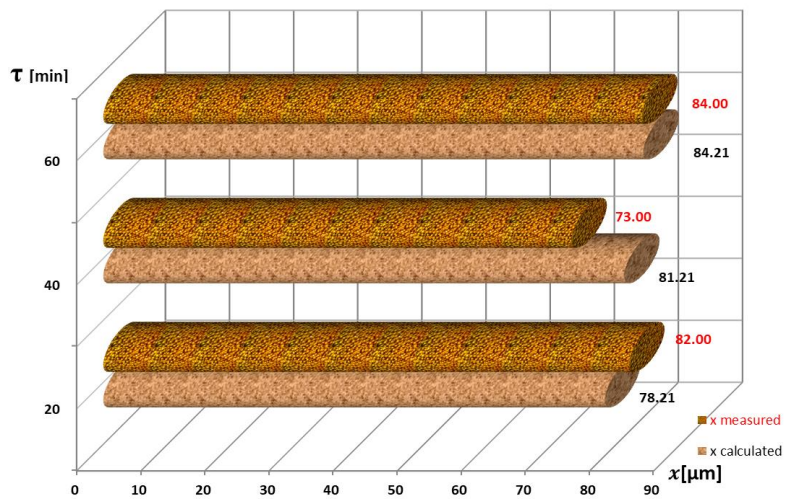
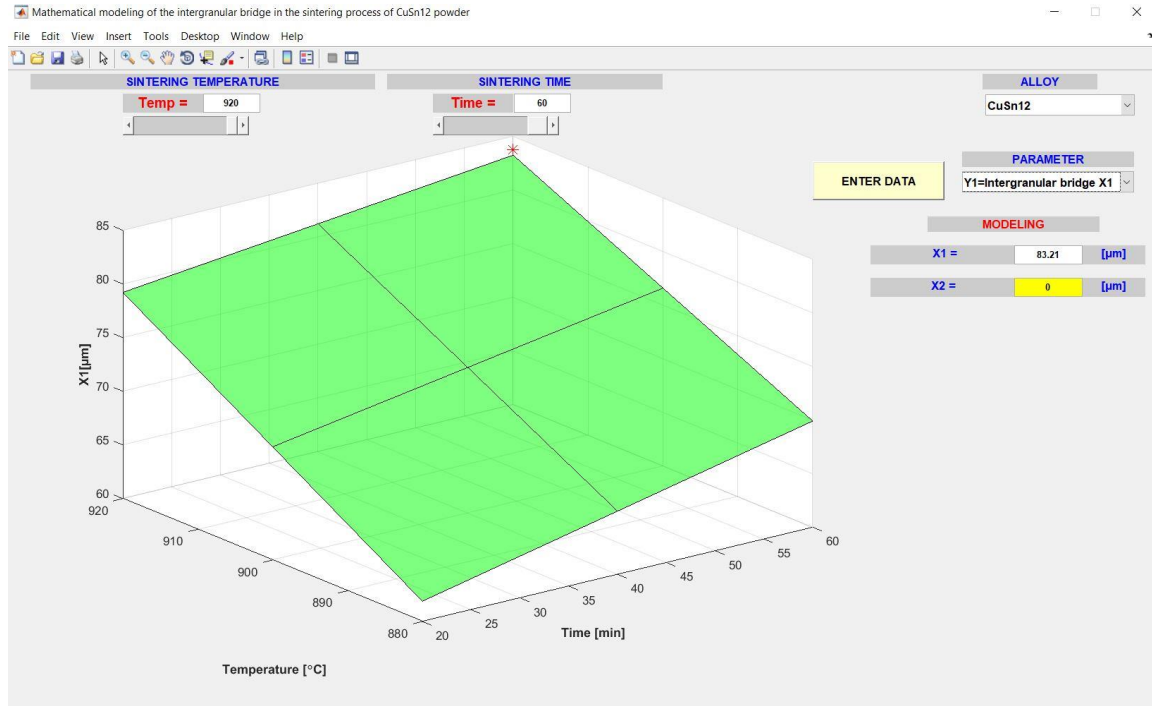


Fig. 13.  $Y_1 = f(\tau)$  for  $t = 920\text{ }^{\circ}\text{C}$



Based on the regression equation of the mathematical model obtained, we created an application in MATLAB R2016a that can make a prediction of the value of the intergranular bridge ( $x$ )

in the range  $t = 880-920$  °C and  $\tau = 20-60$  min. Figures 14 and 15 show some images with simulations performed with this application.



**Fig. 14.** Prediction of the value of the intergranular bridge  $x_1$  for  $t = 920$  °C and  $\tau = 60$  min calculated with the regression equation (8)

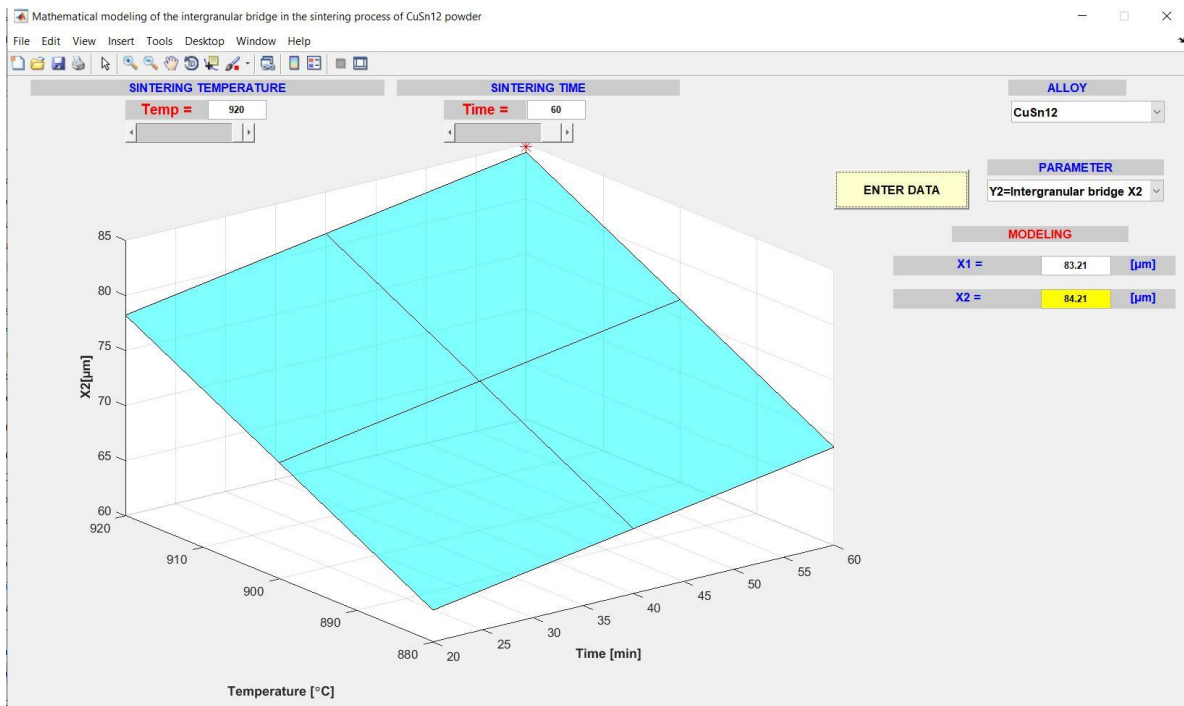


**Fig. 15.** Prediction of the value of the intergranular bridge  $x_2$  for  $t = 920$  °C and  $\tau = 60$  min calculated with the regression equation (13)



#### 4. Conclusions

As can be seen from Tables 10 and 11, the calculated values for the intergranular sintering bridge ( $x$ ) are very close to the measured values, so the first-order mathematical model described by equation (13) allows the simulation of the sintering process of the CSn12 powder, by the variation of the technological parameters,  $t$  and  $\tau$ , within the experienced limits.

It is noted, as expected, the much greater influence of the temperature factor than the time factor on the sintering process, represented by the evolution of the size of the intergranular sintering bridge.

The application made in MATLAB R2016a uses the two forms of the regression equation, (8) and (13) of the obtained mathematical model and can make predictions, with a high probability (>95%) of the size of the intergranular bridge in the interval  $t = 880-920$  °C (with a variation  $\Delta t = 5$  °C) and  $\tau = 20-60$  min (with a variation  $\Delta \tau = 10$  min).

#### References

- [1]. \*\*\*, *Friction Lubrication and Wear Technology*, ASM Handbook, vol. 18, p. 801-811, 1992.
- [2]. \*\*\*, *Powder Metal Technologies and Applications*, ASM Hand Book, vol. 7, p. 343-348, 2572-2599, 1998.
- [3]. Suresh A. L., Mahendran S. K. R., Krupashankara M. S., *Influence of Powder Composition & Morphology on Green Density for Powder Metallurgy Processes*, Int. J. Innov. Res. Sci. Eng. Technol., vol. 04, no. 01, p. 18629-18634, doi: 10.15680/ijirset.2015.0401037, 2015.
- [4]. Sethi G., Upadhyaya A., Agrawal D., *Microwave and conventional sintering of premixed and prealloyed Cu-12Sn Bronze*, Sci. Sinter., vol. 35, no. 2, p. 49-65, doi: 10.2298/SOS0302049S, 2003.
- [5]. Keraghel F., Loucif K., Delplancke M. P., *Study of bronze porous alloy Cu-Sn worked out by metallurgy of the powders*, Phys. Procedia, vol. 21, p. 152-158, doi: 10.1016/j.phpro.2011.10.023, 2011.
- [6]. Jabur A. S., *Effect of powder metallurgy conditions on the properties of porous bronze*, Powder Technol., vol. 237, p. 477-483, doi: 10.1016/j.powtec.2012.12.027, 2013.
- [7]. Nakrod N., McCuiston R., Auechaitanukul C., *Effect of compaction pressure and sintering time on the properties of sintered Cu-10Sn bronze*, Key Eng. Mater., vol. 751 KEM, p. 37-41, doi: 10.4028/www.scientific.net/KEM.751.37, 2017.
- [8]. Cojocaru M. O., Druga L. N., Dragomir D., Tudose F., *Porosity of sintered tin bronzes*, UPB Sci. Bull. Ser. B Chem. Mater. Sci., vol. 79, no. 1, p. 163-172, 2017.
- [9]. Alexandru P., Ștefănescu C., *Experimental Determination of the Kuczynski Equation for the Case of CuSn12 Alloy Sintering*, Ann. "Dunarea Jos" Univ. Galati. Fascicle IX, Metall. Mater. Sci., vol. 45, no. 4, p. 81-86, doi: 10.35219/mms.2022.4.13, 2022.
- [10]. Demian C., Nicoară M., Vida-Simiti I., *Esențial în Metalurgia Pulberilor*, Cluj-Napoca, U.T. Press, 2009.
- [11]. Taloi D., Florian E., Bratu C., Berceanu E., *Optimizarea proceselor metalurgice*, București, Editura Didactică și Pedagogică, 1983.